SAND2018-11771C

Infrared Nanoantenna-Coupled Rectenna for Energy Harvesting

J. Shank **P.S. Davids** **D.W. Peters** **E.A. Kadlec**

Sandia National Laboratories
1515 Eubank SE
Albuquerque, NM 87123
505-845-9347
jshank@sandia.gov

Abstract— **Energy harvesting from relatively low-temperature heat sources is important in applications where long-term power sources are needed such as deep space radioisotope thermoelectric generators (RTGs). Current solutions exhibit low efficiency, require exotic materials and structures, and direct contact to the heat source. While the infrared rectenna is currently low efficiency, the path exists for high-efficiency solid state devices. We have made a scalable design using standard CMOS processes, allowing for large-area fabrication. This would allow devices to be made on the wafer scale using existing fabrication technology. The rectenna has the advantage of using radiated power, thus it does not require direct contact to the hot source, but instead must only view the source. This will simplify packaging requirements and make a more robust system. The devices are monolithic and thus robust to adverse operating environments.**

Here we will discuss the rectenna's physics of operation, particularly light coupling into the structure. Incoming light is coupled to a metal-oxide-semiconductor (MOS) tunnel diode via a broad-area nanoantenna. The nanoantenna consists of a subwavelength metal patterning that concentrates the light into the tunnel diode where the optical signal is rectified. Both the nanoantenna and tunnel diode are distributed devices utilizing the entire area of the surface. The nanoantenna also serves as one contact of the tunnel diode. This direct integration of the nanoantenna and diode overcomes the resistive loss limitations found in prior IR rectenna concepts that resembled microwave rectenna designs scaled down to infrared sizes.

We will show simulation and experimental results of fabricated devices. Simulations of the optical fields in the tunnel gap are illustrative of device operation and will be discussed. The measured infrared photocurrent is compared to simulated expectations. Far-field radiation power conversion is demonstrated using standard radiometric techniques and correlated with the rectified current response. We discuss thermal modelling of the localized heat generation within the rectenna structure to demonstrate the lack of a thermoelectric response. Lastly, we discuss future directions of work to improve power conversion efficiency.

Table of Contents

1. INTRODUCTION 1
2. INFRARED RECTENNA DESIGN 1
3. POWER GENERATION 4
4. DESIGN OPTIMIZATION 5
5. CONCLUSION 8
ACKNOWLEDGEMENTS 8
REFERENCES 8
BIOGRAPHY 9

1. INTRODUCTION

We have recently demonstrated a new device that converts waste heat directly into electrical power [1]. The device, called a rectenna, uses a thermoelectric transduction mechanism based on radiative heat transfer from a hot source to a cooler structured receiver called a rectenna. This new device converts waste heat in the form of infrared radiation directly into electrical power through tunneling rectification.

A key advantage over current thermoelectric power converters is that the rectenna does not require contact with the hot source. Instead a rectenna only needs to see the radiated heat from the source, which results in a robust device with a simplified design. Infrared rectennas can also be designed to operate at longer wavelengths allowing them to produce power from lower temperature sources. The rectenna discussed herein uses standard CMOS materials and processing so that it can be made relatively cheaply, in large-areas, and with high-yield.

Our focus is to increase the power conversion efficiency in order to replace or work in conjunction with conventional thermoelectric materials in radioisotope thermoelectric generators (RTG). A micropower supply based on a rectenna RTG design is anticipated to have a large impact on remote power systems. Any increased efficiency in heat to electrical power conversion will directly lead to a decreased requirement for the amount of a radioisotope thermal source, thus allowing for a smaller lighter-weight power system. Increased robustness to vibration and other adverse environments could also simplify system design.

2. INFRARED RECTENNA DESIGN

Historical Perspective

978-1-5386-2014-4/18/$31.00 ©2018 IEEE

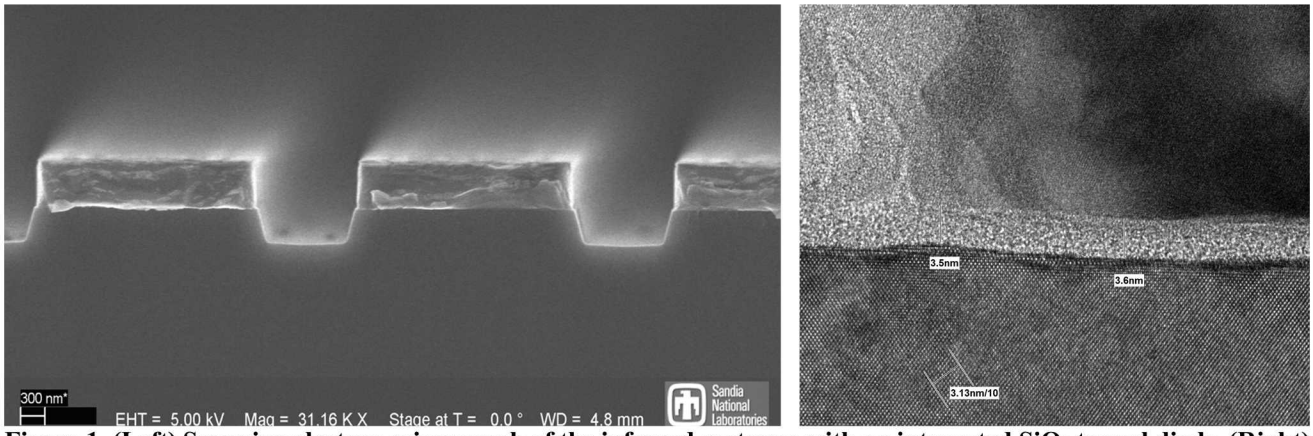

Figure 1. (Left) Scanning electron micrograph of the infrared rectenna with an integrated SiO_2 tunnel diode. (Right) Scanning electron micrograph of the SiO_2 tunnel barrier measuring 3.5-3.6 nm thick.

Rectennas were first developed for microwave power transfer applications in the 1960's by pairing discrete dipole antenna arrays with high speed Schottky diodes [2]. Using narrow-band sources, these early devices were used to demonstrate conversion efficiencies in excess of 90% [3]. In order to achieve these efficiencies, two limitations had to be overcome. First, the RC time constant set by the antenna resistance and diode capacitance had to be reduced such that the rectenna could respond to the microwave frequencies. Second, a high-speed diode was required that could rectify the microwave frequency signal.

These same two problems persist, but are magnified, in designing rectennas capable of responding to infrared radiation [4]. The time constant required for a rectenna to respond to 3 um radiation is 10 femtoseconds. With typical antenna resistances of 100 ohms, this requires a diode capacitance less than 100 attofarads in order to meet the RC time constant requirement. Once parasitic effects are accounted for, the simple pairing of a discrete dipole antenna with a high-speed diode clearly does not meet this requirement. Likewise, the Schottky barrier diodes used at microwave frequencies do not meet the femtosecond speed requirement for infrared frequencies.

In order to meet the time constant requirements for infrared frequencies, the rectenna community has turned to metal-insulator-metal (MIM) tunnel junctions distributed into travelling-wave diodes [5]. With this architecture, both the diode speed requirement can be met using the tunneling mechanism [6] and the diode capacitance can be reduced to the distributed capacitance of the travelling-wave structure [5]. We have expanded this design philosophy and integrated a distributed antenna directly into the distributed travelling-wave tunnel diode [7]. As shown in Figure 1, an aluminum grating antenna is integrated directly onto the MIM tunnel junction with degenerately doped silicon composing the other "metallic" layer.

The experimental device discussed herein was produced using standard CMOS processes for high-yield large-area manufacturing. The minimum lateral feature size is 1.2 um making the device manufacturable even in semiconductor facilities with older photolithography equipment. As shown in Figure 1, the tunnel barrier is approximately 3.5 nm thick, typical of standard CMOS gate oxides.

Additional Physics

While the fully integrated infrared antenna and MIM diode meet the scaled speed requirements of a traditional rectenna design, materials react differently to infrared radiation than microwave radiation requiring the infrared rectenna designer to consider additional physical mechanisms. At microwave frequencies, metals can be considered nearly lossless such that the antenna resistance is dominated by the radiation resistance rather than the ohmic resistance. However, metals at infrared frequencies exhibit losses that must be considered. The integrated antenna architecture addresses this complication by creating a subwavelength structure minimizing the effective length of the antenna.

Such subwavelength structures are commonly used in near perfect absorbers where the reflectance is minimized for a desired wavelength by impedance matching the structure to free space and transmission is minimized by creating material losses at that wavelength [8]. The fully integrated rectenna architecture follows a similar design minimizing the reflection for wavelengths matching the blackbody peak of the desired thermal source. However, instead of adding material losses at this wavelength, the rectenna couples this light into the tunnel diode converting the energy into electrical power.

In addition to material differences, the application of infrared rectennas differs from microwave rectennas. While microwave rectennas typically receive power from an artificial narrow-band source, infrared rectennas must accommodate the bandwidth of a thermal blackbody source.

The peak of this band shifts with temperature such that the infrared rectenna must be designed for a specific application.

Field Enhancement

For a rectenna to produce electrical power the incident radiation must be coupled into the high-speed rectifying diode. The DC power produced by a rectifier is proportional to the diode's asymmetry and is reduced by the diode turn-on voltage. Therefore, operating the rectenna at a voltage past the diode turn-on voltage and at a point with high asymmetry is necessary to produce substantial power. While MIM diodes meet the speed requirements of infrared frequencies, they typically have poor asymmetry at the small voltages developed on an infrared antenna. Therefore, increasing the operating voltage is imperative to obtaining power from an infrared rectenna.

The voltage across an MIM diode can be estimated by the field within the insulating layer multiplied by the thickness of the insulating layer. While the thickness of the tunnel gap cannot be increased dramatically, as it becomes too resistive, the field within the gap can be enhanced [9].

Maxwell's equations dictate that at the interface between two materials the displacement fields normal to the interface will be identical in the absence of a surface charge. Therefore, as shown in Equation 1, the field within the tunnel gap will be inversely proportional to the permittivity of the tunnel gap material as shown in Equation 1 where E_I is the electric field in insulator, E_M is the electric field in the metal, ε_I is the permittivity of the insulator, ε_M is the permittivity of the metal, and ρ_S is the surface charge.

$$\varepsilon_M E_M - \varepsilon_I E_I = \rho_S \qquad \text{Equation 1a}$$

$$E_I = \frac{\varepsilon_M}{\varepsilon_I} E_M + \frac{\rho_S}{\varepsilon_I} \qquad \text{Equation 1b}$$

This interface condition permits the enhancement of the electric field if the permittivity of the tunnel gap material is near zero. For the designed device, silicon dioxide was used as the tunnel gap material with a permittivity near zero at 8 μm as shown in Figure 2.

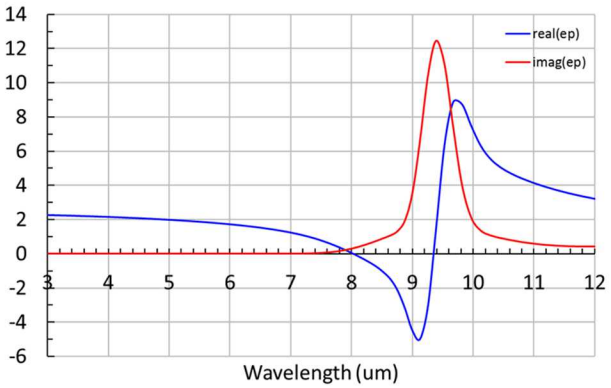

Figure 2: Measured real and imaginary relative permittivity of silicon oxide. The real part of the permittivity approaches zero at 8 um leading to field enhancement.

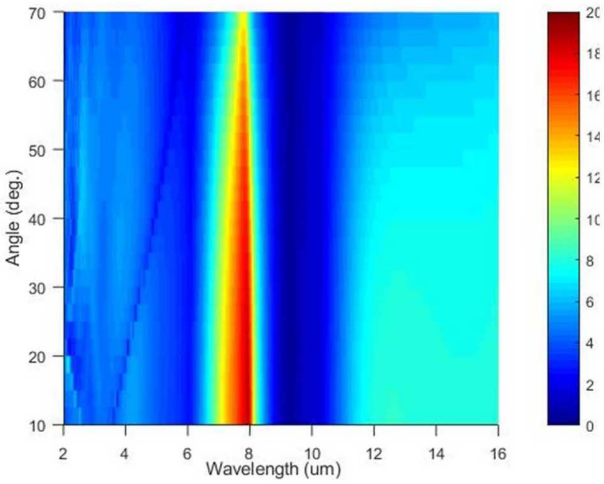

Figure 3: Simulated field concentration in the tunnel gap of the rectenna discussed herein.

While the tunnel gap field enhancement cannot be directly measured, the effect can be simulated to generate expectations for device performance. A model of the fully integrated infrared rectenna was created in COMSOL. As shown in Figure 3, the simulated field in the tunnel gap is nearly 20 times the incident field at 7.9 um.

Light Coupling

In addition to enhancing the electric field within the tunnel diode, it is necessary to couple light into the rectenna to produce power. As discussed in previous work [9], the optical modes present in the rectenna are mixtures of the material dependent epsilon near zero Berreman modes and the structural spoof plasmon modes. These modes are both visible in the reflection maps shown in Figure 4. Good agreement was found between the reflection map simulated in COMSOL and the reflection map measured using hemispherical directional reflectometry (HDR).

As shown in Figure 4, the Berreman mode is observed at high incident angles as a region of low reflectivity around the ENZ wavelength for silicon dioxide at 8 um. This mode is determined by the dielectric material used. In contrast, the spoof plasmon modes appear at low incident angles and are determined by the periodic structure of the rectenna. This mode is shown in Figure 4 as a region of low reflectivity around 6.9 um. Designing the spoof plasmon mode [10] is crucial to achieving power generation from the infrared rectenna.

Figure of Merit

Previous theoretical work determined the single photon tunnel current due to photon-enhanced tunneling within the infrared rectenna [11]. This result is copied below as Equation 2 where $(1\text{-}R^2)$ is the frequency dependent

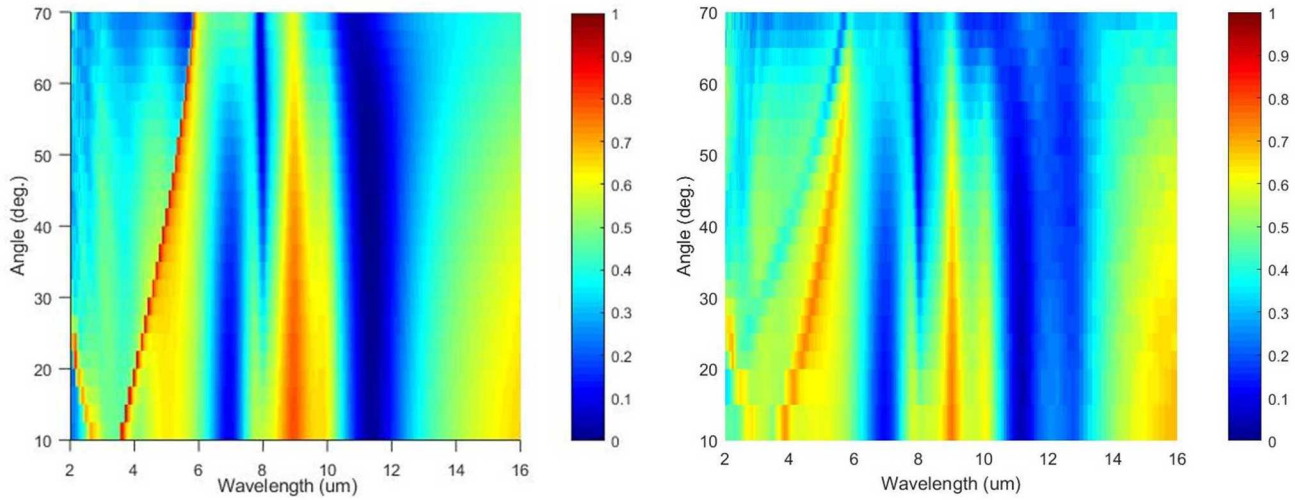

Figure 4. (Left) COMSOL simulated reflection map and (Right) HDR measured reflection map of the infrared rectenna discussed herein.

absorption within the rectenna, γ is the electric field concentration defined as $E_{gap} = \gamma E_o$, $M_\nu^0(T)$ is the incident blackbody spectra exitance, and $T(\nu)$ is the integrated barrier transmission for the tunnel oxide.

$$J^{(1)} = AT^2 \left(\frac{m_r m_l}{m_{ox}^2}\right) 2Z_o \ldots$$

$$\int_\nu \left[(1-R^2)\gamma^2 \left(\frac{qt_{ox}}{h\nu}\right) M_\nu^0(T)T(\nu)\right] d\nu \qquad \text{Equation 2}$$

From this equation for the photon-enhanced tunnel current, a design dependent figure of merit can be produced as Equation 3. This figure of merit is dependent on both the frequency and the angle of the incident light as it includes both the ability of the rectenna to couple light into the tunnel diode and the ability to enhance the electric field.

$$FOM = (1-R^2)\gamma^2 \qquad \text{Equation 3}$$

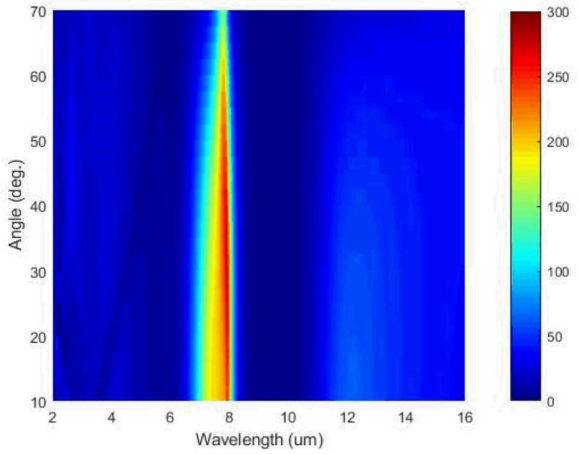

Figure 5: Map of the figure of merit for the infrared rectenna discussed herein.

A map of the figure of merit for the device discussed herein is shown in Figure 5. Power generation occurs due to a narrow band of incident light centered around 7.9 um where both the reflection is low and the field concentration is high. The maximum figure of merit occurs around 27 degrees due to the relatively high reflectivity at near normal angles of incidence.

3. Power Generation

Experimental Results

In order to test the fully integrated rectenna architecture, a small area device (0.15 cm^2) was fabricated. This device was packaged and bonded to a water-cooled block. The rectenna was then illuminated with a blackbody source located 2 mm from the surface of the rectenna. The blackbody temperature was varied from room temperature up to 500°C. The temperature of the rectenna was monitored with a thermocouple bonded to the package of the rectenna and the device temperature never rose above 20°C. At each blackbody temperature, a current-voltage sweep was measured using a Keithley 2400 SMU.

As shown in Figure 6, the open circuit voltage shifts to negative values when illuminated with a blackbody source indicating power generation in the second quadrant, as expected for a rectenna [12]. In addition, the short circuit current rises by several orders of magnitude.

In order to verify that this result corresponds to power generation from the rectenna, the source measurement unit used to measure the I-V characteristics was removed from the circuit and a bank of varying load resistors was added so that the rectenna was the only power source within the system. As shown in Figure 7, the rectenna still produced a measurable voltage across the load resistors when illuminated with a blackbody source. In addition, it was found that the load resistance at the maximum power point matches the

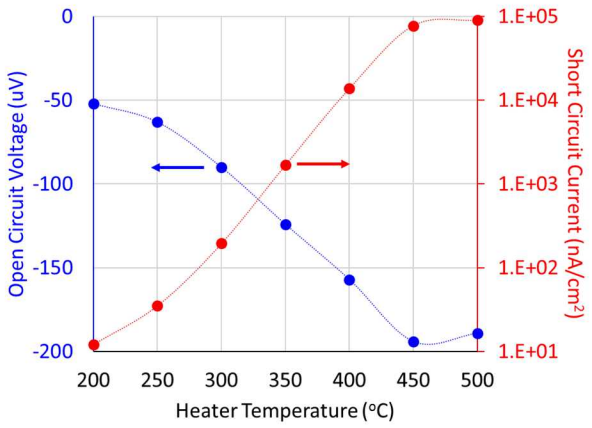

Figure 6: Open circuit voltage and short circuit current of the infrared rectenna as a function of the illuminating blackbody temperature.

rectenna's resistance when illuminated consistent with an impedance matched maximum power transfer condition.

Additional Observations

An additional effect shown in Figure 7 is that under illumination the rectenna becomes significantly more conductive. Temperature dependent I-V measurements performed in the dark indicate that this is not a bolometric effect, but is rather an effect of the illumination. This indicates that while the power generated may be low, there is substantial charge available at the interface that cannot tunnel through the device at the low developed voltages.

One common criticism of infrared rectenna devices is that differentiating between a rectenna response and a thermoelectric response due to localized heating is difficult. While the average temperature of the packaged device does not exceed 20°C, localized heating may still be possible. While the difference between the Seebeck coefficients of aluminum and intrinsic silicon is dramatic, the Seebeck coefficient of degenerately doped silicon is substantially closer to that of aluminum. In order for a thermoelectric response to explain the observed power generation a substantial temperature differential must be sustained across the rectenna.

To address the thermoelectric response of the fully integrated rectenna, the multi-physics capabilities of COMSOL were utilized. Localized device heating was modelled by coupling the electromagnetic simulation to a localized thermal generation physics model. Two thermodynamic situations were simulated. The first simulation assumes good thermal contact between the silicon wafer and the water-cooled package such that the package remains at 300K. The second simulation assumes the rectenna is thermally isolated such that the only temperature loss mechanism is radiation from the front side of the device. Both of these simulations indicate no localized heating such that there is no thermal gradient across the aluminum – silicon oxide - silicon interfaces.

4. Design Optimization

Design Improvements

While the power generated by this initial device (2 nW/cm^2) may be small, there are several aspects of the design that can be improved.

First, efficient power generation occurs when the wavelength of minimum reflection matches the wavelength of maximum field concentration leading to an improvement in the figure of merit. As shown in Figure 8a, the wavelength of minimum reflection scales approximately with the ratio between the antenna width and the cell period. In contrast, as shown in Figure 8b, the wavelength of maximum field concentration

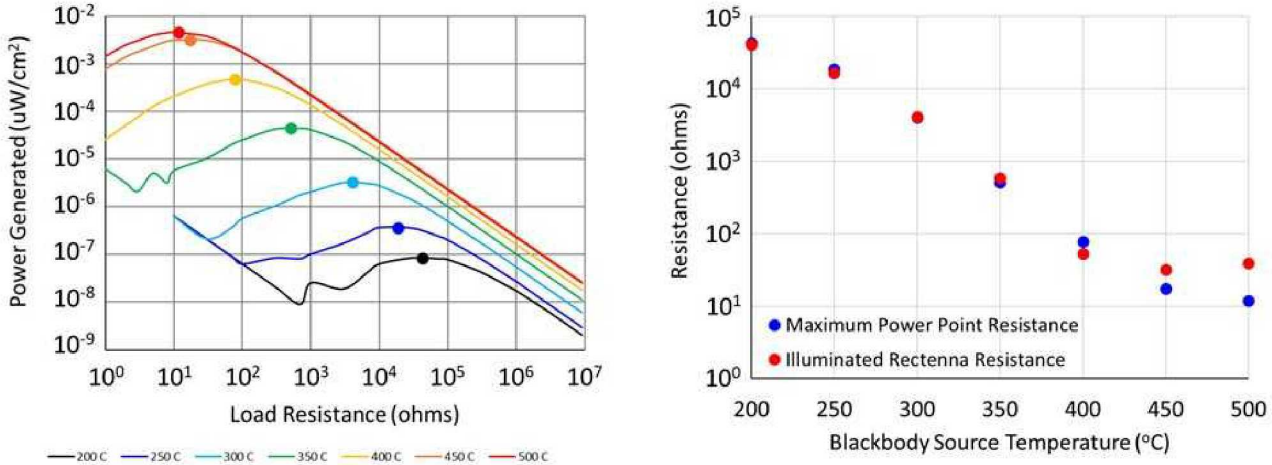

Figure 7. (Left) Power generated by the infrared rectenna as a function of the illuminating blackbody temperature and the load resistance. Dots on the curves correspond to the measured resistance of the rectenna under illumination. (Right) The measured rectenna resistance and the maximum power point load resistance as a function of the illuminating blackbody temperature.

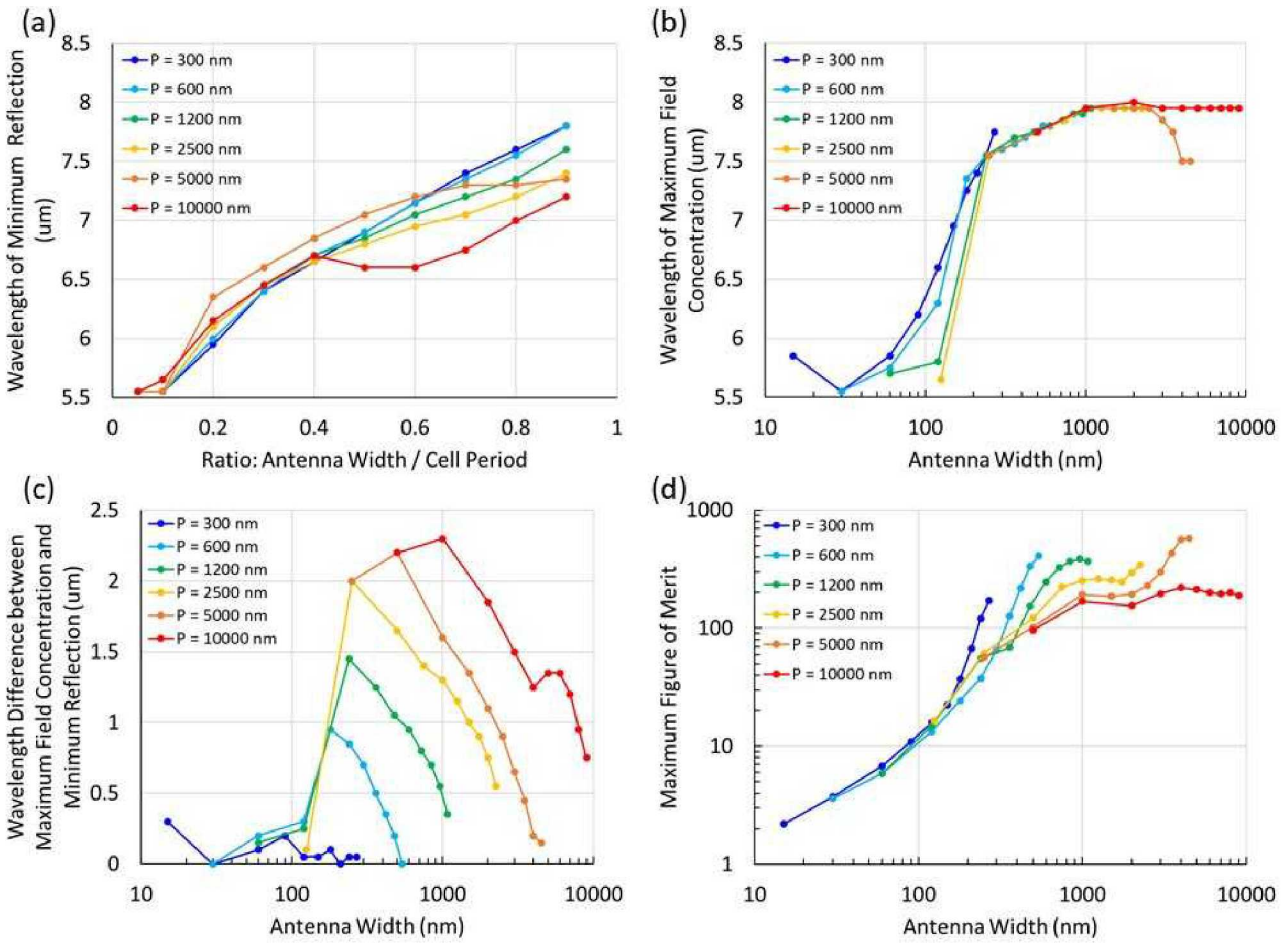

Figure 8. (a) The wavelength of minimum reflection scales roughly with the ratio between the antenna width and the cell period. A deviation from the trend is observed for large rectenna structures that are not subwavelength. (b) The wavelength of maximum field concentration scales roughly with the width of the antenna independent of the cell period. (c) The wavelength difference between the wavelength of minimum reflection and the wavelength of maximum field concentration. Good matching occurs for very small cell periods and for high ratios between the antenna width and the cell period. (d) Optimization of the maximum figure of merit occurs predominately for high ratios between the antenna width and the cell period where both a high field concentration and good matching between the reflection and field concentration spectra occurs.

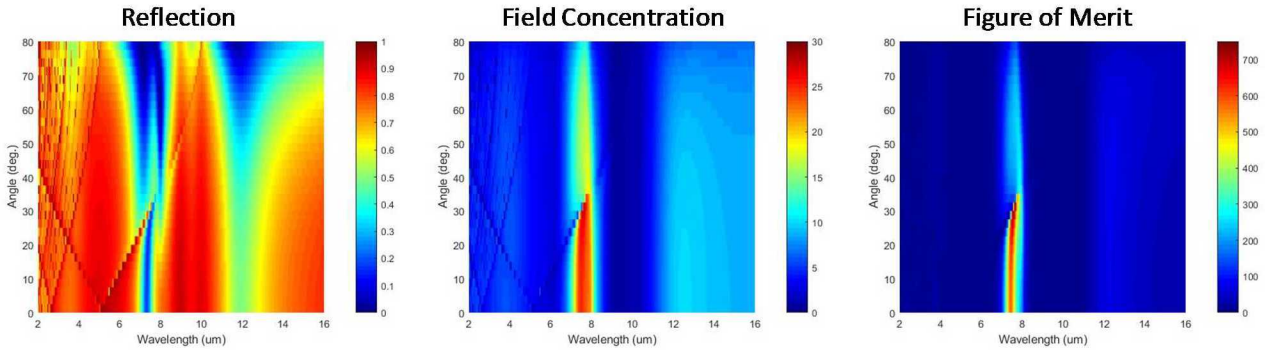

Figure 9. Reflection, Field Concentration, and Figure of Merit maps for an optimized infrared rectenna with a cell period of 5um and an antenna width of 4.5 um

scales approximately with the antenna width. Therefore, the difference between the wavelength of minimum reflection and the wavelength of maximum field concentration can be optimized by engineering the cell period and antenna width. As shown in Figure 8c, this optimization occurs for small cell periods or for high ratios between the antenna width and the

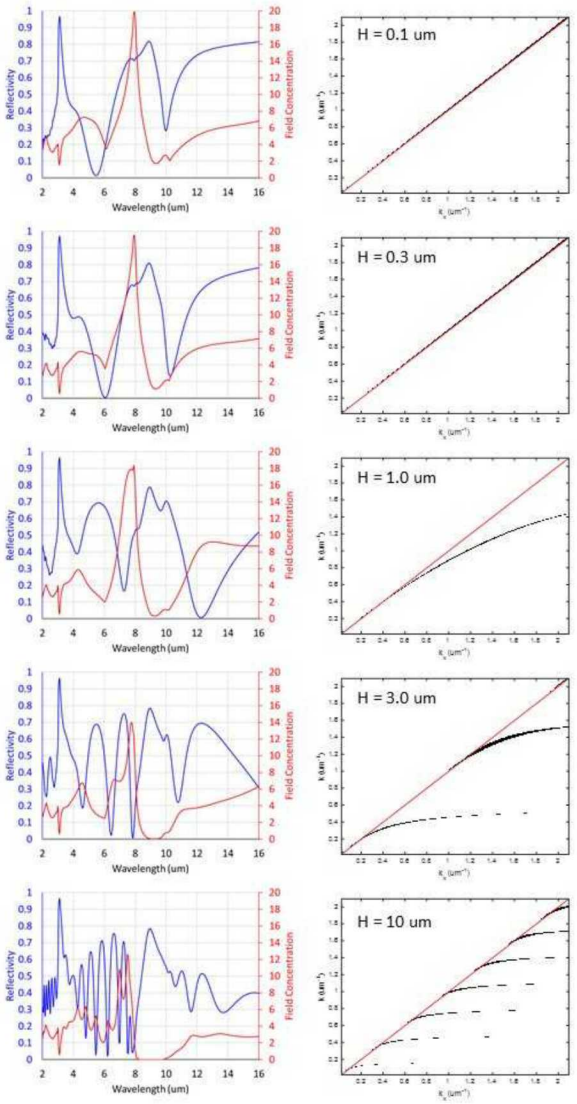

Figure 10: (Left) reflection and field concentration spectra for infrared rectennas with antenna heights of 0.1, 0.3, 1, 3, and 10 um. (Right) spoof plasmon modes for the same structures.

cell period. For small cell periods around 300 nm, the wavelength of minimum reflection and the wavelength of maximum field concentration match for nearly all conditions. However, such small features are difficult to manufacture. In contrast, the wavelength of minimum reflection and the wavelength of maximum field concentration also match for high antenna width ratios even for large cell periods. Such structures are substantially easier to manufacture.

In addition to matching the wavelength of minimum reflection with the wavelength of maximum field concentration, it is important to maximize the figure of merit by having low reflectivity and high field concentrations. As shown in Figure 8d, structures with small cell periods have low figures of merit compared to structures with larger cell periods. This is largely due to higher field concentrations in the larger structures. Likewise, higher figures of merit are achieved for larger antenna widths due to both the higher field concentration and the better matching between reflection and field concentration.

As shown in Figure 9, optimizing the rectenna structure for both the cell period and the antenna width produces a 1.5x improvement in field concentration that is better aligned to the reflection minimum than the experimental device tested herein. This yields a 2.5x improvement in the maximum figure of merit.

While the cell period and the antenna width both impact the figure of merit optimization, the antenna height can also be used to optimize performance. As previously discussed, the reflection spectra are determined by both epsilon near zero Berreman modes and structural spoof plasmon modes. While the ENZ modes are largely independent of the antenna structure, the spoof plasmon modes are heavily dependent on the antenna height.

As shown in Figure 10, for small antenna heights (0.1, 0.3, and 1 um) increasing the antenna height maintains a single spoof plasmon mode. However, as the antenna height increases the wavelength of minimum reflection and the wavelength of maximum field concentration become better aligned improving the figure of merit. In contrast, as the antenna height continues to increase (3 and 10 um) multiple spoof plasmon modes appear creating multiple reflection minima and field concentration maxima that are well aligned. This multi-band approach effectively increases the bandwidth of the infrared rectenna. However, such a design is not without compromise. As shown in Figure 10 and as discussed previously, increasing the antenna height increases the quantity of lossy metal leading to ohmic losses and a decrease in the maximum field concentration. This directly reduces the figure of merit and the ability to produce power. In addition, fabricating such a high aspect ratio antenna would be challenging.

Small structural details can also have a large impact on rectenna performance. As shown in Figure 1, the rectenna tested herein included an overetch into the silicon substrate. This overetch does not substantially change the reflection spectra, but does impact the ability to couple light into the tunnel barrier. As shown in Figure 11, the simulated rectenna without an overetch shows almost 2 times higher field concentration across a wider bandwidth leading to a maximum figure of merit almost 4 times higher than the rectenna with a 200 nm overetch.

Design Alternatives

While the fully integrated infrared rectenna can be further optimized, the design does include some innate limitations. The MIS tunnel diode used herein is a nearly symmetric device at small voltages with a reverse bias current nearly equal to the forward bias current. In order to improve asymmetry either the operating voltage must be increased to where this diode is asymmetric (> 100 mV) or an alternative MIM diode must be used.

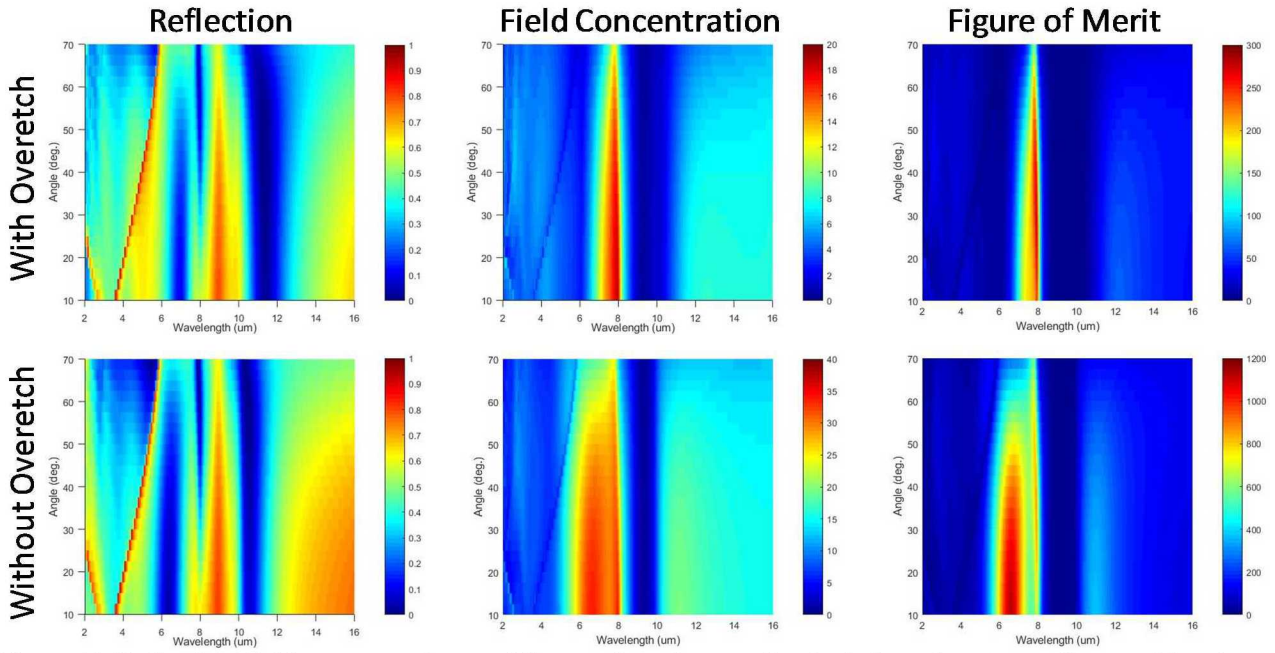

Figure 11. Reflection, field concentration, and figure of merit maps for the infrared rectenna discussed herein and the same structure without overetching into the silicon substrate

The tunnel diode discussed herein uses aluminum and n-type silicon, which have nearly identical workfunctions. Therefore, this device is asymmetric largely because of the asymmetry in the density of states between the aluminum and the silicon rather than their workfunction difference. Most MIM diodes use two metals with differing workfunctions such that the turn-on voltage corresponds to the barrier height between the higher workfunction metal and the insulator's electron affinity. The diode asymmetry then occurs due to Fowler-Nordheim tunneling. While such devices do show improved asymmetry, achieving this asymmetry at low voltages is difficult.

An ideal MIM tunnel diode would have one metal workfunction that exactly matches the insulator's electron affinity. This however is difficult as it requires a low workfunction metal such as an alkali metal [13]. In addition, the silicon – silicon oxide interface used herein is a very clean interface with few defects or trap states. An MIM diode based on Fowler-Nordheim tunneling would have to use less well controlled materials and control of the interfaces would be critical to prevent trap states and Fermi-level pinning.

In addition to changing the rectenna design, other system improvements could increase power generation. The infrared rectenna produces power from a fairly narrow band of wavelengths. However, a thermal blackbody source emits power over a much wider band. While increasing the bandwidth of the infrared rectenna is not practical, a structured emitter placed on the thermal source could narrow the emission bandwidth to match the infrared rectenna. Similar approaches have been used with thermo-photovoltaic systems to improve efficiency [14].

5. Conclusion

The results described in this work demonstrate the potential of infrared rectennas for recovery of waste heat. These devices directly convert infrared radiation into electrical current by concentrating the incident electric field into the gap of a tunnel diode that then rectifies the high frequency field into direct current. Integration of both the antenna and the tunnel diode into a single integrated structure permits the fabrication of relatively inexpensive and large area devices that are robust. The device described herein demonstrated power generation from a low temperature blackbody thermal source.

While the power generated from infrared rectennas remains low, future design improvements are identified that could substantially improve performance.

Acknowledgements

Sandia National Laboratories is a multi-mission laboratory managed and operated by National Technology and Engineering Solutions of Sandia, LLC., a wholly owned subsidiary of Honeywell International, Inc., for the U.S. Department of Energy's National Nuclear Security Administration under contract DE-NA0003525.

References

[1] J. Shank *et al.*, "Power generation from a radiative thermal source using a large-area infrared rectenna," *Physical Review Applied,* vol. 9, no. 5, p. 054040,

2018.

[2] W. Brown and R. George, "Rectification of microwave power," *IEEE spectrum,* vol. 1, no. 10, pp. 92-97, 1964.

[3] W. C. Brown, "Optimization of the efficiency and other properties of the rectenna element," in *Microwave Symposium, 1976 IEEE-MTT-S International*, 1976, pp. 142-144: IEEE.

[4] E. Donchev *et al.*, "The rectenna device: From theory to practice (a review)," *MRS Energy & Sustainability-A Review Journal,* vol. 1, 2014.

[5] S. Grover, O. Dmitriyeva, M. J. Estes, and G. Moddel, "Traveling-wave metal/insulator/metal diodes for improved infrared bandwidth and efficiency of antenna-coupled rectifiers," *IEEE Transactions on Nanotechnology,* vol. 9, no. 6, pp. 716-722, 2010.

[6] A. S. Landsman and U. Keller, "Attosecond science and the tunnelling time problem," *Physics Reports,* vol. 547, pp. 1-24, 2015.

[7] P. S. Davids *et al.*, "Infrared rectification in a nanoantenna-coupled metal-oxide-semiconductor tunnel diode," *Nature nanotechnology,* vol. 10, no. 12, pp. 1033-1038, 2015.

[8] N. Liu, M. Mesch, T. Weiss, M. Hentschel, and H. Giessen, "Infrared perfect absorber and its application as plasmonic sensor," *Nano letters,* vol. 10, no. 7, pp. 2342-2348, 2010.

[9] E. A. Kadlec, R. L. Jarecki, A. Starbuck, D. W. Peters, and P. S. Davids, "Photon-Phonon-Enhanced Infrared Rectification in a Two-Dimensional Nanoantenna-Coupled Tunnel Diode," *Physical Review Applied,* vol. 6, no. 6, p. 064019, 2016.

[10] P. Davids, F. Intravaia, and D. Dalvit, "Spoof polariton enhanced modal density of states in planar nanostructured metallic cavities," *Optics express,* vol. 22, no. 10, pp. 12424-12437, 2014.

[11] P. S. Davids and J. Shank, "Density matrix approach to photon-assisted tunneling in the transfer Hamiltonian formalism," *Physical Review B,* vol. 97, no. 7, p. 075411, 2018.

[12] Z. Zhu, S. Joshi, B. Pelz, and G. Moddel, "Overview of optical rectennas for solar energy harvesting," in *Proc. of SPIE Vol*, 2013, vol. 8824, pp. 88240O-1.

[13] A. Sharma, V. Singh, T. L. Bougher, and B. A. Cola, "A carbon nanotube optical rectenna," *Nature nanotechnology,* vol. 10, no. 12, p. 1027, 2015.

[14] S.-Y. Lin, J. Moreno, and J. Fleming, "Three-dimensional photonic-crystal emitter for thermal photovoltaic power generation," *Applied Physics Letters,* vol. 83, no. 2, pp. 380-382, 2003.

BIOGRAPHY

Joshua Shank *is a Senior Member of the Technical Staff at Sandia National Laboratories. He received his PhD in Electrical Engineering from the Georgia Institute of Technology in 2016.*

Paul S. Davids *received his Ph.D in theoretical condensed matter physics in 1993 from Indiana University while as a graduate research associate in Theoretical Division at Los Alamos National Lab. He was then a post-doc in the Electronics Device and Materials group from 1993-1996. He then joined Intel Oregon and held various research positions from 1996-2008. He joined Sandia National lab in 2008 where he is currently a Principal Member of the Technical Staff. He has over 75 papers and 23 issued patents with 18 pending..*

Emil A. Kadlec *biography not available.*

David W. Peters *is a Principal Member of the Technical Staff at Sandia National Laboratories in the Applied Photonic Microsystems organization. He received his PhD in Electrical Engineering from the Georgia Institute of Technology in 2001. From 2001 to 2004 he was a Director of Central Intelligence Post-Doc at Sandia National Laboratories investigating 2D and 3D photonic crystals. His current interests include the theory, design, and modeling of diffractive optics, plasmonic devices, metamaterials, and metal optics with a focus on infrared detectors and applications.*